Title: Inhibition of BCMA signaling alters protein translation and Multiple Myeloma growth

Authors and Affiliation: Yu Rebecca Miao[1], Can Cenik[2], Dadi Jiang[3], Kazue Mizuno[1], Grace Caiyun Li[1], Hongjuan, Zhao[1,4], Kaushik Thakker[1], Anh Diep[1], Jimmy Yu Xu[1], Xin Eric Zhang[6], Michaela Liedtke[5], Parveen Abidi[5], Wing-sze Leung[1], Albert C. Koong[3], Amato J. Giaccia[1-6]*

[1]Department of Radiation Oncology, Stanford University; Stanford, CA 94305 USA
[2]Department of Molecular Biosciences, University of Texas at Austin; Austin, TX 78712 USA
[3]Department of Radiation Oncology, MD Anderson Cancer Center; Houston, TX 77030 USA
[4]Department of Urology, Stanford University; Stanford, CA 94305, USA
[5]Department of Medicine (Hematology), Stanford University, Stanford, CA 94305 USA
[6]Department of Oncology, Oxford Institute for Radiation Oncology, University of Oxford, Oxford, OX3 7DQ, United Kingdom

Corresponding Author: Amato J. Giaccia, Ph.D.
Director, Oxford Institute for Radiation Oncology
University of Oxford
Old Road Campus Research Building (ORCRB)
Roosevelt Drive
Oxford OX3 7DQ
650.353.1600 (mobile)
44.01865.617030
giaccia@stanford.edu
amato.giaccia@oncology.ox.ac.uk

Conflict of Interest Statement

Authors declare that they have no competing interests.

ABSTRACT

B-cell maturation antigen (BCMA) expression is highly expressed on the surface of MM cells and has been used to target MM tumor cells by CAR-T, Antibody-Drug-Conjugates (ADCs) and BCMA-CD3 bispecific antibodies. However, BCMA is critical for the viability of Multiple Myeloma (MM) tumor cells and to date there have not been any effective therapeutics developed to inhibit BCMA signaling. Here, we investigated the potential of using a soluble BCMA decoy receptor fusion protein (sBCMA-Fc) to trap the BCMA ligands, APRIL and BAFF to achieve ligand mediated BCMA signaling inhibition. Treatment with sBCMA-Fc has proven to be safe and efficacious in inhibiting tumor progression in numerous *in vivo* and syngeneic PDX tumors model. Mechanistically, global ribosome profiling analysis revealed a decrease in the translation efficiency of a subset of proteins in MM cells as a result of BCMA inhibition, indicating that increased BCMA signaling is a driver of dysregulated protein translation in MM cells. In particular, BCMA regulates the translation of ATM interactor (ATMIN/ACSIZ), and inhibition of ATMIN alone reduces the growth of MM cells, supporting its role as a downstream effector of BCMA in promoting MM expansion. Overall, our preclinical and mechanistic data support the concept that inhibition of BCMA signaling through sBCMA-Fc is a viable clinical strategy that alters the protein translation of a subset of proteins that are needed for MM viability and growth.

INTRODUCTION

Multiple Myeloma (MM) remains incurable and despite current therapies, patients often experience treatment relapse and succumb to the disease (1, 2). The development of B-Cell Maturation Antigen (BCMA) directed CAR-T, antibody-Drug Conjugates (ADC) and bispecific have enjoyed considerable clinical success with a subset of patients reporting complete remission post-treatment (3-5). Unfortunately, dose limiting normal tissue toxicity remains a major clinical challenge in this group of patients, which include but are not limited to cytokine storm syndrome, peripheral neuropathy, and ocular toxicity (6-8). Additionally, elderly patients are often excluded from both CAR-T and ADC treatments due to their poor overall health, representing a critically unmet clinical need within this population (9, 10). Therefore, new efficacious therapeutics with favorable safety and tolerability profiles are needed for treating patient's ineligible for both frontline and new investigational MM therapies associated with high drug related toxicity.

B-Cell Maturation Antigen (BCMA) is a member of the TNF receptor family that is uniquely expressed on plasma cells and some differentiated B cells (11, 12). Although widely accepted as a marker of MM and a selective cell surface target for MM targeted therapies, BCMA signaling is also essential for the growth and survival of MM cells (13-15). Upon binding its ligands A proliferation-inducing ligand (APRIL) or B-cell activating factor (BAFF), BCMA promotes AKT, MAPK, and NF-κB signaling, facilitating the transcriptional increase of pro-tumor cytokines that lead to osteoclast mediated bone degradation, cell adhesion and angiogenesis within the tumor niche, promoting MM progression and relapse (16, 17). However, these changes in signaling do not really explain the critical and unique role of BCMA in MM viability. We hypothesize that BCMA is regulating other pathways in MM cells that have yet to be identified and are linked with tolerating high levels of protein production.

Interestingly, while BCMA plays a critical role in MM viability, there are few loss or gain of function mutations identified to date, indicating that BCMA signaling is responsive and dependent to ligand regulation (18). BCMA has two main ligands. The APRIL ligand binds to BCMA with a high binding affinity in a trimeric form and stimulates B cell proliferation and survival. In contrast, BAFF, binds BCMA with a weaker affinity (19). Interestingly, higher serum BAFF levels compared to serum ARPIL levels are found in MM patients, possibly to compensate for its weaker affinity (17, 20). In addition to BCMA, the Transmembrane activator and CAML interactor

(TACI) receptor, which is primarily expressed on mature B-cell and much less so on plasma cells, also binds to APRIL and BAFF, but with a higher binding affinity to BAFF (21). These differences in ligand binding affinities result in discrete biological outcomes (22, 23). As a result, inhibition of TACI signaling (e.g. atacicept) showed modest efficacy in MM but is clinically effective at treating other B-cell related diseases such as IgA Nephropathy (24).

In this study, we devised a ligand neutralization approach, trapping APRIL and BAFF using a Fc-fusion protein consisting of an extracellular domain of BCMA joined to an IgG Fc (sBCMA-Fc) to inhibit BCMA signaling. *In vivo* studies on syngeneic MM mouse models as well as human PDX tumors provides evidence that the addition of sBCMA-Fc treatment can be effectively used as a monotherapy or safely in combination with other MM standard-of-care (SOC) treatments. Specifically, sBCMA-Fc treatment enhanced the anti-tumor efficacy of CD38 antibody and restored bortezomib sensitivity in previously bortezomib resistance MM tumors, suggesting that it could be used to treat both naïve and relapse and refractory (r/r) MM patients. Mechanistically, RPPA analysis suggested that BCMA regulated protein translation. We further investigated this new role of BCMA using ribosome profiling and found that BCMA regulates the translation of subset of cellular proteins that are tightly linked to MM survival (25-28). Together, these studies provide new insight into the role of BCMA in regulating protein translation and how sBCMA-Fc can be safely added to the current SOC for the treatment of MM.

RESULTS

BCMA Signaling is Essential for the Growth and Survival of Multiple Myeloma.

As described above, BCMA expression is significantly elevated in patient myeloma cells compared to healthy plasma cells, making it an attractive target for directed therapies (Fig. 1A). When examining BCMA mRNA expression in a panel of cancer cells originated from different tissue types in the Oncomine database, BCMA was found to be uniquely elevated on MM and B-cell lymphoma, and not detectable in cancer cells other than those of a B cell origin (Sup. Fig. 1A). Higher serum levels of APRIL (Fig. 1B) and BAFF (Fig. 1C) were also found in MM patients, which is consistent with previous reports (29, 30).

To investigate the dependency of MM proliferation on BCMA signaling, we determined the effects of siBCMA knockdown (KD) on MM cell growth in cell culture, we found delayed cell death with siBCMA treatment after 72 hours compared to siCon cells (Sup. Fig 1B), which is consistent with reports in the literature (31). To evaluate the biological outcome of BCMA signaling on established murine MM tumors *in vivo*, we introduced a Tet-off doxycycline-controlled BCMA stable KD system (dox shBCMA) into MM cell lines INA-6 and MM1.R (Sup. Fig. 1C). Induction of shBCMA led to a significant decrease in established INA-6 MM tumor size while mice bodyweight remained unchanged (Fig. 1D, E. Sup. Fig 1D). A second MM tumor model MM1.R showed a similar reduction upon inhibition of BCMA, demonstrating the dependency of BCMA signaling in established MM tumor growth (Sup. Fig 1E, 1F). Tumors harvested from both MM models were assessed for proliferation using Ki67 staining and apoptosis using TUNEL. Decreased Ki67 expression (Fig. 1F, G. Sup Fig. 2A, B) and increased TUNEL signals (Fig. 1H, 1I, Sup. Fig. 2C, D) were observed in both models upon genetic loss of BCMA compared to the tumors harvested from the shSCRM group. Furthermore, the level of human Myeloma protein (paraprotein) secreted by human MM tumor cells was significantly reduced in the mice bearing shBCMA MM tumors, indicative of decreased tumor burden (32) (Fig. 1J). These results establish the therapeutic potential of inhibiting BCMA signaling as a treatment for MM.

Soluble BCMA Decoy Receptor Inhibits APRIL and BAFF Induced BCMA Signaling in MM Cells

Since function mutations in BCMA is uncommon, and BCMA signaling activity is almost entirely regulated by both APRIL and BAFF ligands, we utilized a decoy receptor using the Extracellular Domain (ECD) of the BCMA receptor to block ligand binding. This decoy receptor is fused to a human IgG1 Fc domain (sBCMA-Fc) for improved pharmacokinetic and pharmacodynamic properties (33), effectively inhibiting BCMA ligands APRIL and BAFF mediated BCMA signaling. The use of sBCMA-Fc was previously reported and tested in number of B cell malignancy models as well as solid tumors (34, 35). However, it was not well characterized pharmacologically as a clinically viable candidate to target Multiple Myeloma. Here, we first tested the efficacy of sBCMA-Fc *in vivo* using an Adeno-Associated Virus (AAV) system (Fig. 2A. Sup. Fig. 3A). AAV packaged with mouse sBCMA-Fc or IgG Fc control were administered intravenously into mice on day 2 and day 7 post tumor inoculation (Fig. 2B). Over time, the AAV sBCMA-Fc treated mice harboring MM1.R MM xenografts showed significant delay in tumor growth compared to the IgG Fc controls, supporting the critical roles of APRIL and BAFF in mediating BCMA signaling in MM (Fig. 2C, Sup. Fig. 3B). Based on this proof in principle study, we generated recombinant human sBCMA-Fc protein for a more in depth *in vitro* and *in vivo* characterization (Fig. 2D).

To determine the inhibitory effect of sBCMA-Fc on the viability of MM cell lines, we performed *in vitro* cytotoxicity assays using U266 and MM1.R cell lines. Both cell lines were incubated with 100ng of recombinant hAPRIL to activate BCMA signaling prior to receiving sBCMA-Fc treatment every 48 hours for 7 days. Decrease in MM cell viability was observed when cells were cultured in reduced serum conditions with sBCMA-Fc, suggesting an enrichment of growth factors in the serum can trigger other growth stimulus in MM cells to offset the loss of BCMA signaling. However, this effect is not physiologically relevant and was not observed *in vivo* (Fig 2E). Apoptosis of MM cells post sBCMA-Fc treatment was visualized through electron microscopy and occurred in a dose dependent manner (Fig 2F). In summary, sBCMA-Fc effectively neutralized both APRIL and BAFF binding to BCMA *in vivo* and *in vitro* and treatment can lead to MM cell apoptosis.

To determine the pharmacokinetic profile of sBCMA-Fc, we administered a single dose of 10 mg/kg of fluorescently labeled sBCMA-Fc into non-tumor bearing mice. Based on changes in signal intensity over time, we determined that the half-life of sBCMA-Fc is approximately 24 hours in mice, consistent with other soluble receptors (Fig. 3A). Additionally, serum levels of

mouse APRIL (Fig. 3B top) and BAFF (Fig. 3B bottom) were quantified after administering a single dose of 10 mg/kg sBCMA-Fc. We observed an almost 72 h inhibition of serum BAFF levels compared to a 20 h inhibition of APRIL levels. Most importantly, these results confirm that human sBCMA-Fc can effectively sequester mouse APRIL and BAFF in circulation and can be used for *in vivo* testing. In addition, non-tumor bearing mice were dosed with sBCMA-Fc at 10mg/kg every 48 hours for 28 day and no significant tissue toxicity, changes in body weight, or hematological changes were found (Fig. 3C, D. Sup. Table 1), providing evidence that sBCMA-Fc can be safely dosed *in vivo* without significantly toxicity concerns. In contrast, treatment with sBCMA-Fc resulted in significant tumor reduction in both MM1.R and INA-6 MM tumor models (Fig. 3E, F) and was associated with decreased tumor cell proliferation (Fig. 3G, I) and increased apoptosis (Fig. 3H, J). Collectively, these findings provide evidence that the sBCMA-Fc is safe and efficacious as a monotherapy in numerous xenograft models of MM.

sBCMA-Fc is a Clinically Relevant Therapeutic Candidate for the Treatment of Multiple Myeloma

To further validate the therapeutic potential of sBCMA-Fc in human multiple myeloma specimens, we established human PDXs models of MM by engrafting freshly isolated human MM cells into the tibia of immunodeficient murine host (Sup. Fig. 4A). MM cells from two patients (patient no. 3 and 5) were successfully propagated for *in vivo* testing. After inoculation of PDX derived MM cells and confirming increased levels of human M protein (IgGκ) in mouse serum (Fig. 4A), we initiated sBCMA-Fc treatment. CT scans on animals with successful engraftment showed macroscopic osteolytic lesions that are consistent with osteopenia found in MM patients (Fig. 4B). Engrafted mice were dosed with 10 mg/kg doses of sBCMA-Fc every 48 hours for 28 days and tumor growth was evaluated by detecting human IgGκ in blood until mice reached a terminal endpoint (Fig.4 C, D, Sup. Fig. 4B, C). Treatment with sBCMA-Fc led to a significant reduction in tumor progression, IgGκ signals and prolonged overall survival in two PDX lines that were successfully propagated, demonstrating that BCMA signaling in human MM cells remains ligand dependent.

We also evaluated the relevance of sBCMA-Fc in different combination therapies. The combination sBCMA-Fc with a CD38 therapeutic antibody (αCD38) was tested in the MM1.R tumor model and showed superior anti-tumor activity compared to single treatment of either

monotherapy alone (Fig 4E, F). There were no differences in bodyweight among the treatment groups, indicating that this combination therapy is not result in additional normal tissue toxicity (Fig. 4G). Clinically, the heterogeneous nature of MM often leads to the emergence of therapeutically resistant clones in many MM patients (36, 37). Therefore, we investigated whether therapeutic inhibition of BCMA signaling can benefit patients with acquired resistance to bortezomib, a proteasome inhibitor currently used in frontline MM therapy. To test this hypothesis, we developed a panel of bortezomib resistant MM cell lines generated through continuously exposing parental MM cells to increasing concentrations of bortezomib. Over time, this treatment resulted in more than a 3-fold increase in resistance to bortezomib compared to their parental counterparts (Fig. 4H). Interestingly, MM cells resistant to bortezomib showed elevated BCMA expression, suggesting a potential association between BCMA signaling and bortezomib resistance that warrants further investigation (Fig. 4I).

In vitro cytotoxicity assays demonstrated enhanced survival of bortezomib resistant MM cells compared to its parental control (Sup. Fig. 5A, B), treatment with sBCMA-Fc alone resulted in a significant growth inhibition of bortezomib resistant MM cells, supporting the link between BCMA signaling and bortezomib resistance (Sup. Fig. 5C). Importantly, the combined treatment of bortezomib and sBCMA-Fc was highly effective in killing bortezomib resistant MM cells, suggesting that the addition of sBCMA-Fc can re-sensitize bortezomib resistant cells to bortezomib treatment (Sup Fig. 5D). I*n vivo*, bortezomib resistant MM1.R MM cells were subcutaneously inoculated into NSG mice and treated with vehicle, sBCMA-Fc at 10mg/kg every 48 hours, daily dosing of bortezomib at 0.5mg/kg or the combination of two treatments. Animals were sacrificed when tumor size reached ethical limits. Consistent with *in vitro* analysis, animals which received combination treatment showed a significant survival advantage, with 80% of animals remaining disease free up to 100 days (Fig. 4J). Treatment with sBCMA-Fc improved the median survival from 35 days to 67 days. As expected, bortezomib treatment of the resistant MM tumors failed to show therapeutic benefit when compared to the control. In summary, by using different clinically relevant MM models, we found that sBCMA-Fc is safe and efficacious as a monotherapy or can be combined with current standard of care treatments to enhance therapeutic efficacy without additional toxicity.

Ribosome Profiling Reveals Distinct Changes in Protein Translation Upon BCMA Signaling Alteration

Although inhibition of BCMA signaling through ligand neutralization is effective in inhibiting MM growth and viability, the underlying mechanism responsible for this is unclear. While MM cells treated with sBCMA-Fc showed a reduction in signaling pathways associated with MAPK and AKT signaling, those pathways are shared by many receptors and are not unique to MM. Interestingly, sBCMA-Fc treatment led to a general reduction in mTOR protein translation signaling after treatment (Sup Fig 6A). However, genetic knockdown of BCMA in MM cells U266 using siBCMA further revealed robust changes in the key regulators of protein translation and synthesis such as EIF family member eIF4E, suggesting a potential link between BCMA signaling and protein translation (Fig. 5A, Sup. Fig. 6B, RPPA Data Table S2). To investigate whether BCMA acts as a regulator of protein translation globally or selectively, we performed ribosome profiling on U266 cells with siScramble or siBCMA knockdown. Ribosome profiling is a specialized analysis method that provides quantitative measures of gene-specific translation efficiency (Fig. 5B). Technically, mRNA fragments protected by ribosomes were isolated and sequenced, and in the same population of cells total RNA abundance is quantified by RNA-Seq (38). We performed extensive quality control analysis of the ribosome profiling data using the RiboR (39) and observed the expected three nucleotide periodicity, enrichment of footprints in coding regions and the expected signals at the translation start and stop sites (Sup. Fig. 6C-E). Spearman correlation analysis showed a robust correlation between all samples except for BCMA Scramble 3 (RPF3), which was removed from analysis to retain the quality and consistency of the reads (Sup Fig. 6F, G).

Changes in total mRNA serves as a reference for analyzing ribosome bound mRNA associated changes in translation efficiency (Sup. Fig. 7A, B). Ingenuity Pathway Analysis (IPA) identified mTORC1 mediated signaling as the top canonical pathway altered upon the loss of BCMA signaling activity, a finding consistent with western blotting analysis performed earlier (Sup Fig. 6A, B). In addition, GeneGo MetaCore^{TM} analysis also revealed enrichment in the protein translation associated eIF2 signaling pathway as a process networks altered upon loss of BCMA (Fig. 5D). Subsequently, we calculated changes in translation efficiency when controlling for differences in total mRNA expression (Fig. 5E) (40). Through gene enrichment analysis using the REACTOME pathway database, we found enriched gene signatures associated with initiation and elongation of protein translation (Fig. 5F-H). Furthermore, pathways that are responsible for the synthesis of both large and small ribosome subunits were also decreased in siBCMA MM cells,

suggesting a potential role of BCMA signaling in ribosome biogenesis (Fig. 5I). Collectively, these data suggest that BCMA signaling in MM cells maybe a selective regulator of protein translation.

BCMA Signaling Regulates ATMIN Expression by Modulating Translation Efficiency

Upon sBCMA-Fc treatment, we observed a decrease in the translation efficiency of a subset of cellular proteins and focused on one protein in particular, ATMIN (ASCIZ) (Fig. 6A). Since recent studies shows ATMIN and its binding partner Dynein light chain regulates the development of B cell malignancies (41-44), we investigated the role of ATMIN in MM. While initially discovered as an ATM interacting protein, ATMIN is often associated with ATM-mediated signaling and recruitment of 53BP1 upon DNA damage (45-47). Since RPPA showed no changes in DNA damage signaling proteins upon BCMA loss (Sup Fig. 7C), we hypothesized that altered ATMIN expression may not be a result of DNA damage response but instead modulated by BCMA (Sup. Fig 7C, Sup. RPPA Data Table S2). We performed polysome fractionation to validate BCMA mediated translational changes in ATMIN expression. Ribosomes captured from MM cell lysates were separated into pooled fractions of heavy polysomes, lighter ribosomes and monosomes to determine which fractions bound ATMIN upon the loss of BCMA expression (Fig. 6B). When compared to the control, siBCMA expressing MM cells showed significantly decreased ATMIN transcript binding to heavy polysomes, indictive of reduced ATMIN translation efficiency (Fig. 6C). In addition, ATMIN is exclusively regulated at the translational level by BCMA since total ATMIN mRNA transcripts remain unchanged upon the loss of BCMA expression (Fig. 6D).

To directly access changes in ATMIN after BCMA inhibition with siRNA, we compared ATMIN protein levels in MM cells treated with siScrambled controls to two different siBCMA molecules and found strong inhibition of ATMIN protein by both siBCMAs compared to siScrambled (Fig. 6D). Finally, to determine the effect of ATMIN on cell viability, we generated two independent CRISPR knockout cell lines in U266 cells and found a 30-40% reduction in cell viability, suggesting that ATMIN is an important translational target of BCMA but there are additional translational targets of BCMA that may contribute to MM viability.

DISCUSSION

The activation of the BCMA pathway by its ligands, APRIL and BAFF, provides pro-survival signals and promotes MM progression (17, 30). Developing therapeutic antibodies against BCMA receptor alone or its primary ligand APRIL and BAFF have proven to be challenging for treating MM (16). We believe two major issues may contribute to their limited success. First, therapeutic antibodies with nanomolar binding affinity often do not possess sufficient affinities required to disrupt the interaction between the native APRIL/BCMA binding, which is known to be in picomolar range. Second, APRIL neutralizing antibodies are not designed to block the interaction between BAFF and BCMA and thereby present a means of maintaining BCMA signaling in MM when APRIL levels are decreased.

To overcome these problems, we used a soluble BCMA decoy receptor that acts as a ligand trap for both APRIL and BAFF ligands. The use of sBCMA-Fc to inhibit BCMA signaling was first published in 2000 and was tested in colorectal and lung tumor models with different levels of efficacy (35). This was an interesting finding, but in surveying tumors of different histology and origins (Sup. Fig. 1A), APRIL and BAFF are the most strongly upregulated in MM and this is where one would expect a sBCMA-Fc molecule to be the most effective. Interestingly, testing of a sBCMA-Fc has never made it into the clinic for either lung or colorectal cancer. In this study, the soluble decoy receptor approach allows us to take advantage of high binding affinity between APRIL and BCMA which cannot be achieved with therapeutic antibodies against BCMA or APRIL. In addition, sBCMA-Fc also inhibits BAFF *in vivo* (Fig 3B). Interestingly, atacicept, a decoy receptor derived from a soluble form of another APRIL and BAFF binding TNF receptor TACI, only showed modest clinical efficacy as a treatment for Multiple Myeloma (48). This can be explained that TACI expression is associated with mature B-cells but shows bimodal expression pattern in Multiple Myeloma cell lines (49). The major difference between BCMA and TACI binding to APRIL and BAFF are their ligand binding affinities, and affect B cells at different developmental stages (50). Number of studies have reported different binding affinities between APRIL and BAFF to BCMA and TACI (21, 51, 52). However, it was somewhat consistent that has BCMA has highest binding affinity to APRIL with measured K_D between 30 to 300pM, while binding affinity between BAFF and BCMA is reported to be significantly lower in the μM range (52). In contrast, TACI preferentially bind to BAFF with a KD of approximately 150 pM and APRIL at approximately 1 nM (19). Importantly, *in vivo* pharmacodynamic studies showed

complete suppression of serum APRIL and BAFF levels in mice upon administering a single dose of sBCMA-Fc at 10mg/kg. Suggesting that sBCMA-Fc is equally capable of inhibiting both human and mouse derived APRIL and BAFF. Consistent with these findings, sBCMA-Fc mediated suppression of APRIL and BAFF led to the inhibition of BCMA signaling in MM tumors, effectively reducing tumor growth in both xenograft and PDX models. Furthermore, the addition of sBCMA-Fc to bortezomib treatment can effectively re-sensitize bortezomib resistant MM cells both *in vitro* and *in vivo*, significantly prolonging the overall survival of mice bearing bortezomib resistant tumors without additional toxicity. Results from these studies provided sound preclinical rationale demonstrating that the ligands mediated neutralization of BCMA signaling is a clinically feasible approach for targeting both naïve and treatment resistant MM.

Mechanistically, we discovered that BCMA acts as a regulator of protein translation governing a subset of cellular proteins. We used ribosome profiling to survey the global translational landscape of MM cells upon the loss of BCMA. This strategy revealed distinct proteins that were post-transcriptionally controlled which otherwise would not be detected by measuring total mRNA transcripts (40, 53). Specifically, we found enrichment in pathways that governs protein translation machineries, including translation initiation, elongation, and ribosome integrity. Protein translation is a highly regulated given its essential role in every cellular process, this is especially true for plasma cells, which serves as a power house of immunoglobulin production (54). The inhibition of BCMA resulted in the reduction of Ig immunoglobulins, which at high levels, is clinically associated with infections, peripheral neuropathy and bone damages in MM patients (32, 55).

When ribosomes bound mRNA fragments are sequenced and mapped to its corresponding total mRNA transcriptome, one can numerically quantify the translation efficiency of the protein of interest. We found that ATMIN (ATM-interacting protein, ASCIZ) was one of the proteins that is strongly associated with changes in translation efficiency after BCMA inhibition. Although ATMIN is implicated in the DNA damage response (46), we found that it is also regulated by BCMA in a DNA damage independent pathway. In B cells, ATMIN can interact with dynein light chain subunit (Dynll1) in an ATM independent manner (42, 43) and recent reports indicate that ATMIN and Dynll1 are involved in the development of B-cell lymphoma, providing a link between dysregulated B cell development and ATMIN signaling in MM (42). Inhibition of ATMIN reduced MM cell survival, but did not completely phenocopy the inhibition of BCMA,

indicating that there maybe multiple downstream effectors of BCMA that are important for MM viability.

In conclusion, based on *in vitro* and *in vivo* characterization, we propose that the intervention of BCMA signaling in MM can be safely and efficaciously achieved through the use of sBCMA-Fc to neutralize APRIL and BAFF mediated BCMA activation. Furthermore, we identified a molecular link between BCMA signaling and protein translation machinery, contributing to the fundamental understanding of the biological consequences associated with BCMA signaling. In addition, we found ATMIN as a downstream translational target of BCMA signaling which is important for cell viability. Considering the current clinical challenges associated with MM treatment, we believe sBCMA-Fc is a viable clinical strategy that can be safely deployed as a treatment for Multiple Myeloma or added on to current SOC without additional toxicity.

MATERIAL AND METHODS

Study Approval

This study was designed to characterize the biological functionality of BCMA signaling during MM progression. All Multiple Myeloma patient specimens were collected from Multiple Myeloma patients treated at Stanford Cancer Center under the approval of Stanford IRB No.13535. Healthy blood specimens were obtained from Stanford Blood Center. *In vivo* animal studies were conducted under the approval of AAAPLAC at Stanford University. Sample sizes for animal were determined based on power calculations previously conducted *in vivo* studies. All animals were randomly assigned to treatment groups. Samples were not excluded from studies except for animals that required early termination due to unforeseeable illness that are unrelated to the study. Endpoints of experiments were defined in advance for each experiment. Tumor growth curves were presented for studies where tumor growth was measurable, serum levels of Myeloma protein levels were used as a marker of tumor progression in orthotopic PDX model and Kaplan-Meier analysis were used to define survival advantages in the sBCMA, bortezomib combination study. Appropriate statistical analysis was used for each experimental study.

Cell Lines

Human MM cell lines U266, MM1.R, INA6 and RPMI-8226 cells were maintained in RPMI-1640 media supplemented with 10% fetal bovine serum (FBS) and 1% Penicillin/Streptomycin in standing flasks and a humidified 37 °C, 5% CO_2 incubator. INA6 Cells were supplemented with 2ng/ml of human IL-6 to maintain its growth. All cell lines were generously gifted by Dr. Albert Koong and Dr. Dadi Jiang at the Department of Radiation Oncology, MD Anderson (Houston, TX). Isolation of B-cells from healthy donor and MM patients were performed using EasySep™ Human B-Cell Isolation Kit according to manufacturer's protocol (Cat. No. 17954, Stemcell Technologies, Vancouver, Canada).

RNA Library Preparation

Briefly, snap frozen cell pellets (100 million cells per sample) were lysed in polysome lysis buffer (20 mM Tris-HCl pH 7.5, 250 mM NaCl, 15mM MgCl2, 1mM DTT, 0.5% Triton X-100, 0.024 U/ml TurboDNase, 0.48 U/ml RNasin, and 0.1 mg/ml cycloheximide). Lysates were centrifuged for 10 minutes at 4C, 14,000 x g. The supernatant was used for the isolation of ribosome bound

mRNA, and total mRNA sequencing. SUPERase-In (0.24U/ml) was added to the lysate used for polysome fractionation to prevent RNA degradation.

Ribosome Sequencing Analysis

The sequencing files for ribosome profiling and RNA-Seq data were processed using RiboFlow (39). All source code is freely available at https://github.com/ribosomeprofiling. Briefly, 3' adapter sequence (AAAAAAAAAA) was removed from all reads using cutadapt. The 5' end of each read includes 3 bases from the template switching reaction and also removed before alignment. We used a sequential alignment strategy to first filter out rRNA and tRNA mapping reads followed by mapping to representative isoforms for each as defined in the APPRIS database (56). Next, PCR duplicates were removed from the ribosome profiling data using the 5'end of the sequence alignment coordinates. Finally, the resulting information was compiled into a .ribo file (39) for downstream analyses.

Bioinformatic Analysis

All statistical analysis were carried using RiboR (39). For quantification of ribosome occupancy, footprints of length between 26 and 30 (both inclusive) nucleotides were used. Metagene plots were generated using the 5' end of each ribosome footprint. Ribosome occupancy and RNA-Seq data was jointly analyzed, and transcript specific dispersion estimates were calculated after TMM normalization (57). To identify genes with differential translation efficiency, we used a generalized linear model that treats RNA expression and ribosome occupancy as two experimental manipulations of the RNA pool of the cells as previously described (40). The model was fit using edgeR (57) and p-values were adjusted for multiple hypothesis testing using Benjamin-Hochberg correction.

We used an adjusted p-value threshold of 0.05 to define significant differences. R packages cowplot, pheatmap, EnhancedVolcano, ggpubr, ggplot2, and reshape2 were used for analyses and plotting (58).

Establishing MM PDX Models Using MM Patient Specimens

Mononuclear cells were isolated from bone marrow aspirate of Multiple Myeloma patients and inoculated into the left tibia of 5-6 weeks NSG mice. Injection path into the tibia was established

using an empty needle penetrating through the tibia bone guided by X-ray, then the empty needle is removed, and X-ray turned off to avoid MM cells exposing to radiation. Patient cells were inoculated using a fresh needle and syringe. MM tumor growth was monitored by serum level of human IgG (M) protein. Once the host mice showed successful engraftment marked by increase of serum human IgG level, the animal was sacrificed, bone marrow flushed, and mononuclear cells collected for intratibial injection into 2 host mice. This process is repeated until sufficient N number is reached for each study. 11 patient samples were inoculated, 2 patient samples were successfully propagated for *in vivo* studies.

Establishment of Bortezomib Resistant MM Cell Lines

Bortezomib (Cat no. S1013, SelleckChem, TX) resistant U266, MM1.R and INA6 cells were established by continuous incubation with increasing doses of bortezomib starting from 1nM, to 3, 4, 5, 7, 8 and 10nM. Full recovery of cell viability is confirmed prior to increasing bortezomib to the next dose.

***In vivo* Studies**

All animal experiments were reviewed and approved by the Institutional Animal Care and Use Committee (IACUC) at Stanford University. Female NOD-*scid* gamma mice age 6-8 weeks were purchased from the Jackson Laboratory (Stock no. 005557) and used for all *in vivo* analysis throughout the study. Mice were housed in pathogen-free animal facility, kept under controlled environment with 12 h light-dark cycles. For INA6 d MM1.R and MM1.R bortezomib resistant tumor studies (dox-inducible, AAV and sBCMA-Fc), $10x10^7$ cells were injected subcutaneously with 50% growth factor reduced Matrigel (Cat. no. 356230, Corning, NY). Bodyweight and tumor growth were measured 3 times a week until study termination. Animals were terminated upon subcutaneous tumor reaches ethical termination point. For PDX studies, non-terminal bleeding was performed on animals every 14 days for evaluating serum M protein as markers of tumor progression. Animals were terminated once shown signs of physical distress. sBCMA-Fc were manufactured by Chempartner Shanghai (Shanghai, P.R. China), daratumumab (Cat no. A2027) and bortezomib (Cat no. S1013) were both purchased from SelleckChem (Houston, Tx).

Polysome Analysis

U266 cells were transfected with siScramble and siBCMA as described. Cells were pelleted and lysed in buffer (20 mM Tris-HCl, pH 7.4, 100 mM NaCl, 5 mM $MgCl_2$, 1 mM DTT, 1 % Triton X-100, 0.1 % NP-40, 100 µg/ml CHX, 20 U/ml TurboDNase I, complete protease inhibitor EDTA-free) in nuclease-free water. After lysis, RNA concentrations were measured using Nanodorop UV spectrophotometer and normalized amounts of RNA were layered onto a sucrose gradient (25-50% sucrose (w/v), 20 mM Tris-HCl, pH 7.4, 100 mM NaCl, 15 mM $MgCl_2$, 100 µg/ml CHX) in nuclease-free water and centrifuged in a SW41Ti rotor (Beckman) for 2.5 hr at 40,000 rpm at 4°C. Sixteen fractions were collected by the Density Gradient Fraction System (Brandel). To each fraction, 0.1 ml of 10 % SDS was added and mixed. 0.1 ml of 3 M NaOAc, pH 5.5 and 0.1 ml of water were added to each SDS containing fraction. For normalization, 500 pg of bioistronic firefly luciferase mRNA was added to each fraction.

Total RNA from each fraction was extracted using acid-phenol:chloroform. Briefly, to each fraction, 900 µl of acid-phenol:chloroform was added and mixed thoroughly. The mixture was heated at 65 °C for 5 min, and centrifuged at 21,000 g for 10 min, RT. The aqueous phase (700 µl) was removed and precipitated overnight at -80 °C with 700 µl isopropanol and 1.5 µl GlycoBlue Coprecipitate (Invitrogen). The samples were centrifuged at 21,000 g, 30 min, 4 °C, supernatant was discarded, and the RNA pellet was washed twice with 500 µl cold 75 % ethanol. Pellets were dried for 15 min, RT and resuspended in nuclease free water. Total RNA from each fraction was treated with 2 U/µl TurboDNase I, incubated at 37 °C for 30min and column purified using the RNA Clean and Concentrator-5 (Zymo) according to the manufacturer's instructions. RNA was eluted in 6 µl, twice. Except for the first fraction (F1), RNA was pooled from every three subsequent fractions (F2-4, F5-7, F8-10, F11-13, F14-16) and measured using Nanodorop UV spectrophotometer.

For RT-qPCR, 600 ng of purified RNA was used for reverse transcription with the iScript supermix (Bio-Rad) according to the manufacturer's instructions. (Please see qRT-PCR protocol for primer sequences)

Statistical Analysis

All cell number, tumor volume, survival and quantification of *in vivo* and *in vitro* studies were conducted using GraphPad Prism software (GraphPad Software Inc, CA). ANOVA with Tukey-

Kramer test was used for comparing multiple treatment groups with each other. $P < 0.05$ was considered significant. Repeated measure ANOVA was used for comparing multiple treatment groups measured over time. Statistical analysis of survival curves was conducted for the survival studies. A log-rank (Mantel-Cox) test was performed to compare mean survival among groups; $P \leq 0.05$ was considered statistically significant.

AUTHORS CONTRIBUTIONS

Conceptualization: YRM, CC, DJ, KM, EXZ, ML, PA, ACK, AJG

Methodology: YRM, CC, DJ, KM, GCL, HZ, KT, ML, PA, AL

Investigation: YRM, CC, DJ, KM, GCL, HZ, KT, AD, JX, EXZ

Fund acquisition: AJG

Project administration: YRM AJG

Supervision: YRM, ACK, AJG

Writing: YRM, CC, DJ, AJG

ACKNOWLEDGMENTS

The authors wish to thank Drs. Vignesh Viswanathan, Dhanya Nambiar, Quynh-Thu Le for sharing experimental reagents. We would like to thank Stanford microscopy facility for electron microscopy imaging, Stanford virus core facility for the production of AAV virus, Stanford animal facility for maintaining animal colonies, Chempartner Shanghai for the production of sBCMA-Fc and Biacore™ analysis, TB-seq for the isolation and preparation of ribosome bound mRNA and the University of Delaware sequencing facility for running ribosome sequencing.

FIGURES AND FIGURE LEGENDS

Figure 1

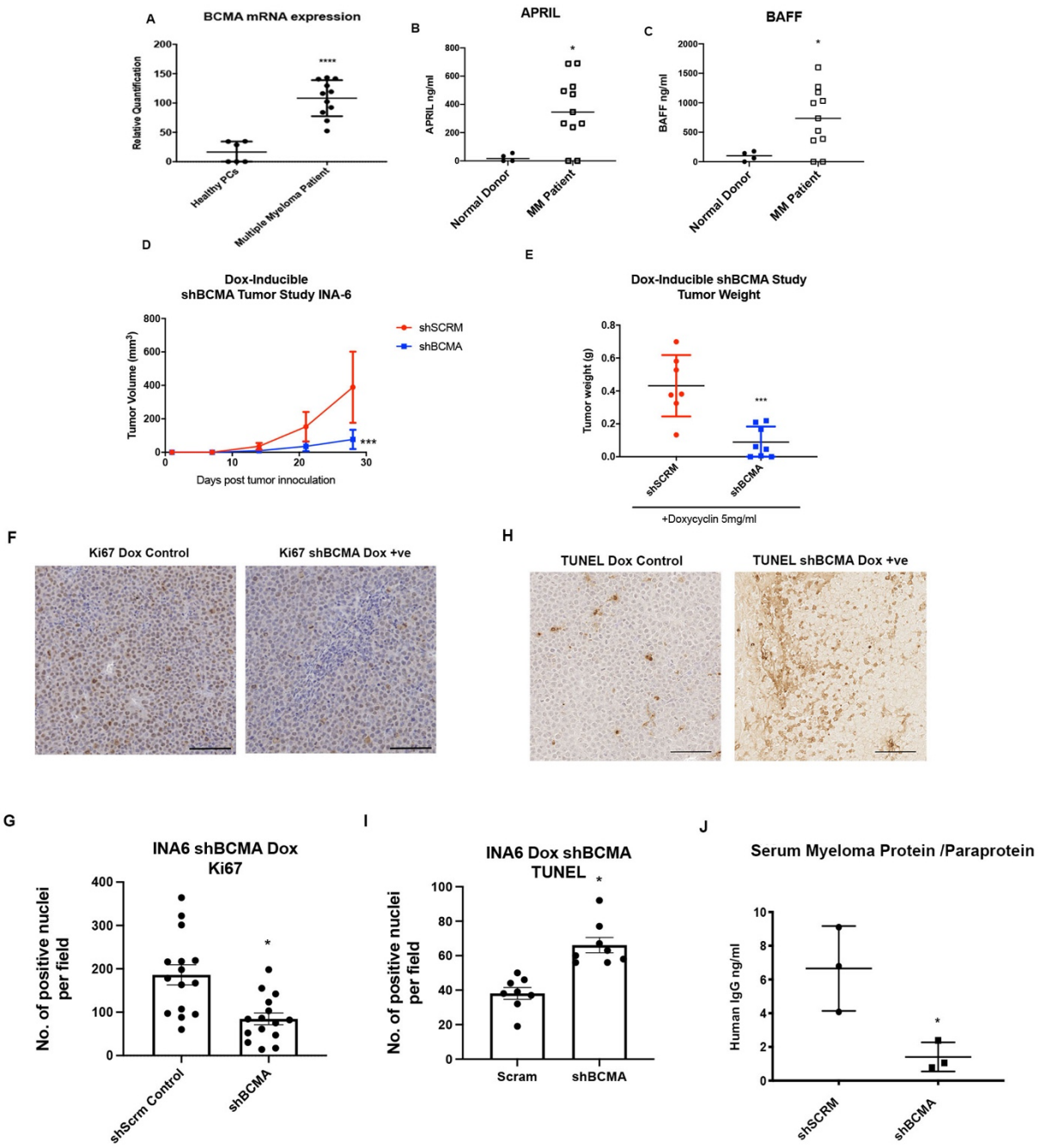

Figure 1: BCMA and its ligands APRIL and BAFF are upregulated in MM and support the growth and survival of MM *in vivo*. (A) BCMA mRNA transcript validated in patient myeloma cells (N=11) and plasma cells harvested from healthy donors (N=6). **(B)** Serum APRIL level detected in MM patients (N=11) compared to healthy donors (N=4) through ELISA. **(C)** Serum BAFF level detected in MM patients (N=11) compared to healthy donors (N=4) through ELISA. **(D)** Subcutaneous tumor growth of INA-6 MM cells with stably transfected doxycycline-inducible BCMA KO shRNA (N=8) or scramble shRNA (N=7) in 6 weeks old female NSG mice. **(E)** Comparing tumor weights of terminally harvested mice inoculated with doxycycline-inducible shSCRM (N=7) and shBCMA (N=8) in INA-6 MM tumor cells. **(F)** Representative images of Ki67 positive cells in the harvested tumors of doxycycline-inducible shSCRM and shBCMA analyzed by IHC staining. Scale bar 50µm. **(G)** Quantitative analysis of Ki67 positive cells in the harvested tumors of doxycycline-inducible shSCRM and shBCMA, represented as the average number of positive nuclei per image field. **(H)** Representative images of TUNEL positive cells in the harvested tumors of doxycycline-inducible shSCRM and shBCMA analyzed by IHC staining. Scale bar 50µm. **(I)** Quantitative analysis of TUNEL positive cells in the harvested tumors of doxycycline-inducible shSCRM and shBCMA, represented as the average number of positive nuclei per image field. **(J)** Total Human M protein (Paraprotein) detected in the serum of NSG mice inoculated with doxycycline-inducible shSCRM and shBCMA human INA-6 MM tumor cells harvested terminally (N=3). Statistical analysis was conducted using One-way ANOVA for comparing between treatment groups and repeated ANOVA for changes occur over time. P value *=<0.05, **=<0.01. ***=<0.001.

Figure 2

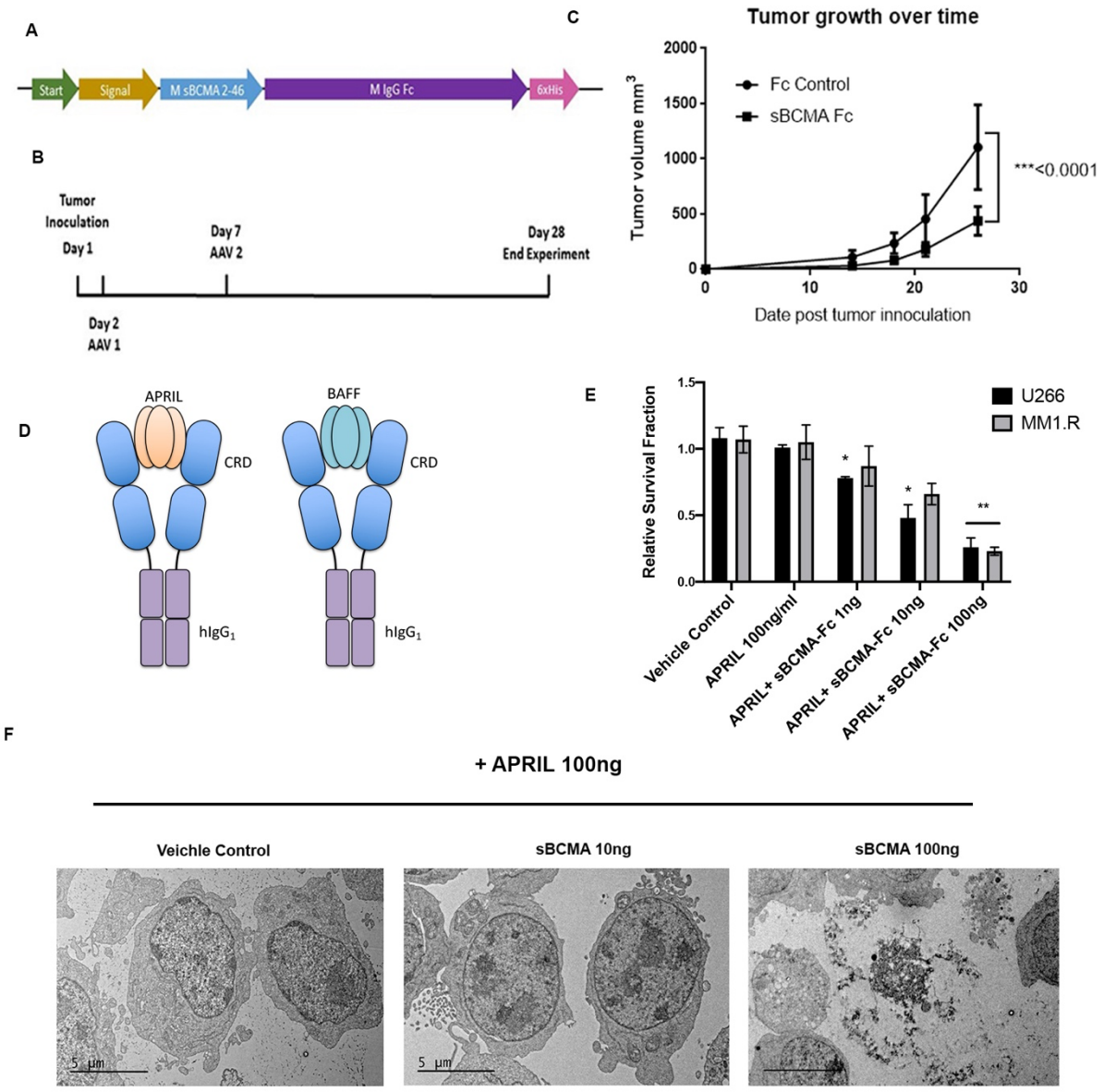
A
Start
Signal
M sBCMA 2-46
M IgG Fc
6xHis
B
Tumor Inoculation Day 1
Day 7 AAV 2
Day 28 End Experiment
Day 2 AAV 1
C
Tumor growth over time
Fc Control
sBCMA Fc
Tumor volume mm3
Date post tumor innoculation
***<0.0001
D
APRIL
BAFF
CRD
hIgG1
E
U266
MM1.R
Relative Survival Fraction
Vehicle Control
APRIL 100ng/ml
APRIL+ sBCMA-Fc 1ng
APRIL+ sBCMA-Fc 10ng
APRIL+ sBCMA-Fc 100ng
F
+ APRIL 100ng
Veichle Control
sBCMA 10ng
sBCMA 100ng
5 µm

Figure 2: Soluble BCMA decoy receptor as a targeted treatment through neutralizing APRIL and BAFF. (A) Illustrative design of AAV virus construct expressing mouse soluble BCMA amino acid no. 2 to 46 fused with mouse IgG Fc. **(B)** Schematic protocol of AAV dosing in animals inoculated with MM1.R MM tumors. **(C)** Subcutaneous tumor growth of MM1.R MM cells in mice dosed with AAV sBCMA-Fc (N=8) and AAV Fc control (N=8) in 6 weeks old female NSG mice. **(D)** Schematic illustrations of recombinant human sBCMA-Fc binding to human ARPIL and BAFF. **(E)** sBCMA-Fc dose-dependent, cytotoxicity assay validating the *in vitro* cell survival in the presence of increasing doses of sBCMA-Fc and hAPRIL (100ng/ml) in U266 and MM1.R MM cells. Cells were maintained in a low 3% FCS to reduce possible growth stimulation mediated through other growth factors present in FCS. Each sample was performed in triplicates. **(F)** Representative Transmission Electron Microscopy images of U266 MM cells treated with vehicle control, sBCMA-Fc 10ng/ml and sBCMA-Fc 100ng/ml in the presence of hAPRIL (100ng/ml). Scale bar 5μM. Statistical analysis was conducted using T test and one way ANOVA for comparing between treatment groups. Repeated ANOVA used for changes in tumor growth over time. P value *=<0.05, **=<0.01. ***=<0.001.

Figure 3

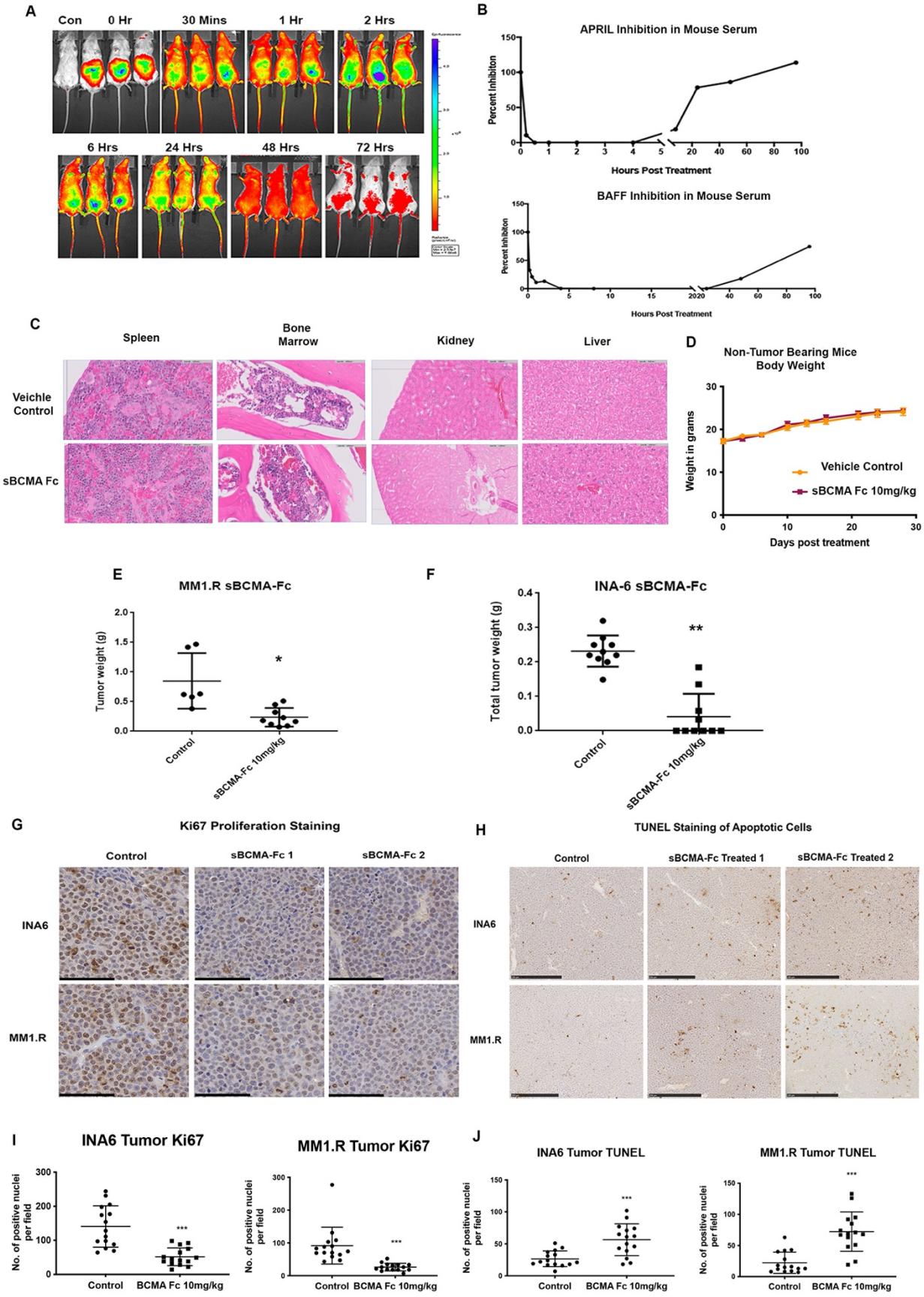
A
Con
0 Hr
30 Mins
1 Hr
2 Hrs
6 Hrs
24 Hrs
48 Hrs
72 Hrs
B
APRIL Inhibition in Mouse Serum
Percent Inhibiton
Hours Post Treatment
BAFF Inhibition in Mouse Serum
Percent Inhibiton
Hours Post Treatment
C
Spleen
Bone Marrow
Kidney
Liver
Veichle Control
sBCMA Fc
D
Non-Tumor Bearing Mice Body Weight
Weight in grams
Vehicle Control
sBCMA Fc 10mg/kg
Days post treatment
E
MM1.R sBCMA-Fc
Tumor weight (g)
Control
sBCMA-Fc 10mg/kg
F
INA-6 sBCMA-Fc
Total tumor weight (g)
Control
sBCMA-Fc 10mg/kg
G
Ki67 Proliferation Staining
Control
sBCMA-Fc 1
sBCMA-Fc 2
INA6
MM1.R
H
TUNEL Staining of Apoptotic Cells
Control
sBCMA-Fc Treated 1
sBCMA-Fc Treated 2
INA6
MM1.R
I
INA6 Tumor Ki67
MM1.R Tumor Ki67
No. of positive nuclei per field
Control
BCMA Fc 10mg/kg
J
INA6 Tumor TUNEL
MM1.R Tumor TUNEL
No. of positive nuclei per field
Control
BCMA Fc 10mg/kg

Figure 3: sBCMA-Fc treatment effectively inhibits tumor growth in murine models of MM. **(A)** Pharmacokinetic analysis of sBCMA-Fc labeled with Alexa Fluor® 488 after given a single dose of 10mg/kg IP were imaged over time. **(B)** Serum level of APRIL (top panel) and BAFF (bottom panel) in mouse blood after a single dose of sBCMA-Fc at 10mg/kg given ip. Each data point represents the mean of two animals collected at the same time point. **(C)** Representative H & E staining images of organ tissues harvested from non-tumor bearing mice treated with sBCMA-Fc at 10mg/kg every 48 hours for 28 days. Stained sections were analyzed by a board-certified veterinary pathologist. Scale bar 100μm. **(D)** Changes in bodyweight of non-tumor bearing mice treated with sBCMA-Fc. **(E)** Terminal tumor weight of mice inoculated with MM1.R MM tumors and treated with vehicle control or 10mg/kg of sBCMA-Fc. **(F)** Terminal tumor weight of mice inoculated with INA-6 MM tumors and treated with vehicle control or 10mg/kg of sBCMA-Fc. **(G)** Representative images of Ki67 positive cells in the vehicle control and sBCMA-Fc treated INA-6 (top panels) and MM1.R (bottom panels) MM tumors analyzed by IHC staining. Scale bar 50μm. **(F)** Representative images of TUNEL positive cells in the vehicle control and sBCMA-Fc treated INA-6 (top panels) and MM1.R (bottom panels) MM tumors analyzed by IHC staining. Scale bar 50μm. **(I)** Quantification of Ki67 staining. **(J)** Quantification of TUNEL staining. Statistical analysis was conducted using T test and one way ANOVA for comparing between treatment groups. Repeated ANOVA used for changes in tumor growth over time. P-value *=<0.05, **=<0.01. ***=<0.001.

Figure 4

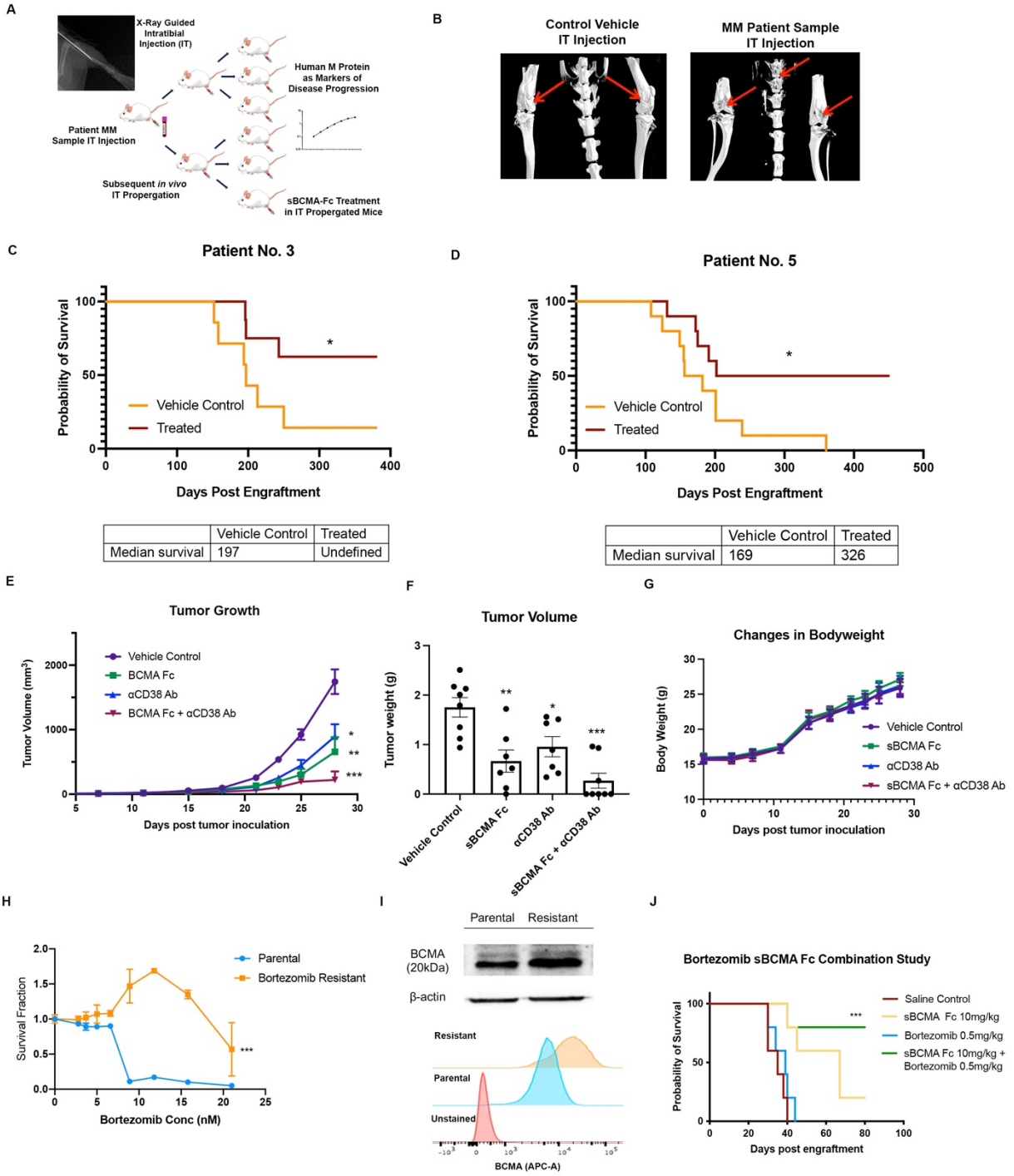

	Vehicle Control	Treated
Median survival	197	Undefined

	Vehicle Control	Treated
Median survival	169	326

Figure 4: sBCMA-Fc is a clinically relevant MM treatment as a monotherapy or can be safely used in combination with SOC. (A) Schematic illustrations of *in vivo* MM PDX propagation. Patient tumor cells were isolated from patient bone marrow biopsies and injected into the tibia of the NSG mice. PDX were subsequently propagated *in vivo* using the same intratibial inoculation procedure and treated with vehicle control or sBCMA-Fc. Human IgG protein in mouse serum is continuously monitored over time as a marker of tumor progression. **(B)** Representative CT scans of mice tibias, femurs and vertebrates inoculated with control (left) or MM PDX tumor cells (right). Osteolytic bone degradation was observed in MM PDX injected animal (red arrows on the right image) but not in the control injected animals (red arrows on the left image). **(C)** Kaplan Meier survival analysis of animals engrafted with MM cells from patient no. 3 showing prolonged overall survival in sBCMA-Fc treated group (N=8) compared to the vehicle control (N=7). Medium survival (in days) shown below. **(D)** Kaplan Meier survival analysis of animals engrafted with MM cells from patient no. 5 showing prolonged overall survival in sBCMA-Fc treated group (N=10) compared to vehicle control (N=10). Medium survival (in days) shown below. **(E)** Subcutaneous tumor growth of MM1.R MM cells in mice dosed with sBCMA-Fc 10 mg/kg every 48 hours (N=7), αCD38 10mg/kg weekly (N=7), sBCMA-Fc and αCD38 combination (N=8) and vehicle control (N=8) in 6 weeks old female NSG mice. **(F)** Terminal tumor weight from study described in (E). **(G)** Changes in bodyweight of animals from study described in (E) and (F). **(H)** *In vitro* cell survival analysis of U266 bortezomib resistant cells treated with 10nM of bortezomib in combination with increasing doses of sBCMA-Fc over time. Each data points represent technical triplicate of a single experiment. **(I)** BCMA protein expression in bortezomib resistant MM cells evaluated through western blotting (top panel) and flow cytometry (bottom panel). **(H)** Kaplan Meier survival plot of NSG mice orthotopically inoculated with MM1.R MM tumors and treated with vehicle control, sBCMA-Fc 10mg/k, bortezomib 0.5mg/kg and combination of sBCMA-Fc 10mg/kg and bortezomib 0.5mg/kg. sBCMA-Fc were dosed IP every 48 hours and bortezomib were dosed via oral gavage daily. Animals terminated once tumor reaches ethical end point. Statistical analysis was conducted using One-way ANOVA for comparing between treatment groups and repeated ANOVA for changes occur over-time. Kaplan Meier estimator was calculated for survival curves. P-value *=<0.05, **=<0.01. ***=<0.001

Figure 5

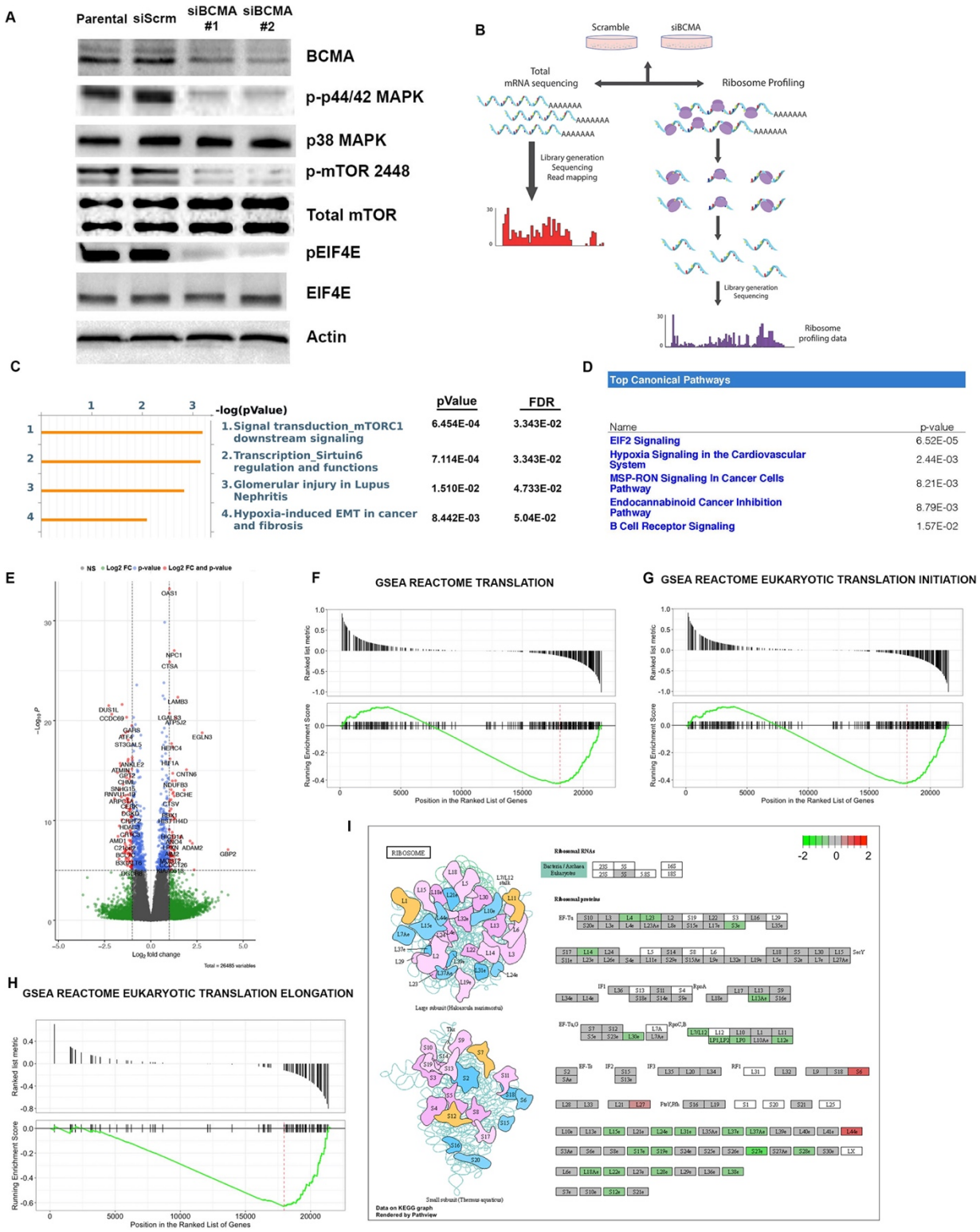
A
Parental
siScrm
siBCMA #1
siBCMA #2
BCMA
p-p44/42 MAPK
p38 MAPK
p-mTOR 2448
Total mTOR
pEIF4E
EIF4E
Actin
B
Scramble
siBCMA
Total mRNA sequencing
Ribosome Profiling
Library generation Sequencing Read mapping
Library generation Sequencing
Ribosome profiling data
C
-log(pValue)
pValue
FDR
1. Signal transduction_mTORC1 downstream signaling 6.454E-04 3.343E-02
2. Transcription_Sirtuin6 regulation and functions 7.114E-04 3.343E-02
3. Glomerular injury in Lupus Nephritis 1.510E-02 4.733E-02
4. Hypoxia-induced EMT in cancer and fibrosis 8.442E-03 5.04E-02
D
Top Canonical Pathways
Name p-value
EIF2 Signaling 6.52E-05
Hypoxia Signaling in the Cardiovascular System 2.44E-03
MSP-RON Signaling In Cancer Cells Pathway 8.21E-03
Endocannabinoid Cancer Inhibition Pathway 8.79E-03
B Cell Receptor Signaling 1.57E-02
E
NS Log2 FC p-value Log2 FC and p-value
Log2 fold change
F
GSEA REACTOME TRANSLATION
Ranked list metric
Running Enrichment Score
Position in the Ranked List of Genes
G
GSEA REACTOME EUKARYOTIC TRANSLATION INITIATION
H
GSEA REACTOME EUKARYOTIC TRANSLATION ELONGATION
I
RIBOSOME
Data on KEGG graph
Rendered by Pathview

Figure 5: Ribosome profiling identifies BCMA as a master regulator of protein translation machinery in MM. (A) Western blotting analysis of changes in protein expression associated with protein translation upon genetic knockdown using siBCMA. **(B)** Schematic illustration of ribosome profiling workflow. **(C)** MetaCore analysis revealing top changes in process networks based on Gene Ontology with P-value and FDR**. (D)** Ingenuity Pathway Analysis of RNA-seq data showing top five significantly changed canonical pathways. **(E)** Volcano plot analysis of global changes in protein translation upon loss of BCMA expression in MM. Not significant (gray), significant changes in Log_2FC value (green), significant changes in p-value (red) and significant changes in both p-value and log_2FC (red) are presented according to color coding. Left side of the volcano plots shows decrease in target expression upon loss of BCMA, the right side shows negative correlation upon loss of BCMA. GSEA REACTOME enrichment analysis showing enriched signatures in associated with protein translation **(F)**, eukaryotic translation initiation **(G)** and eukaryotic translation initiation upon BCMA loss **(H)**. **(I)** Graphic illustration of large ribosome subunits (top) and small ribosome subunits (bottom). Each subunit showing changes in translation abundance upon BCMA loss. Decreased expression (green), no change (gray) or increased expression (red).

Figure 6

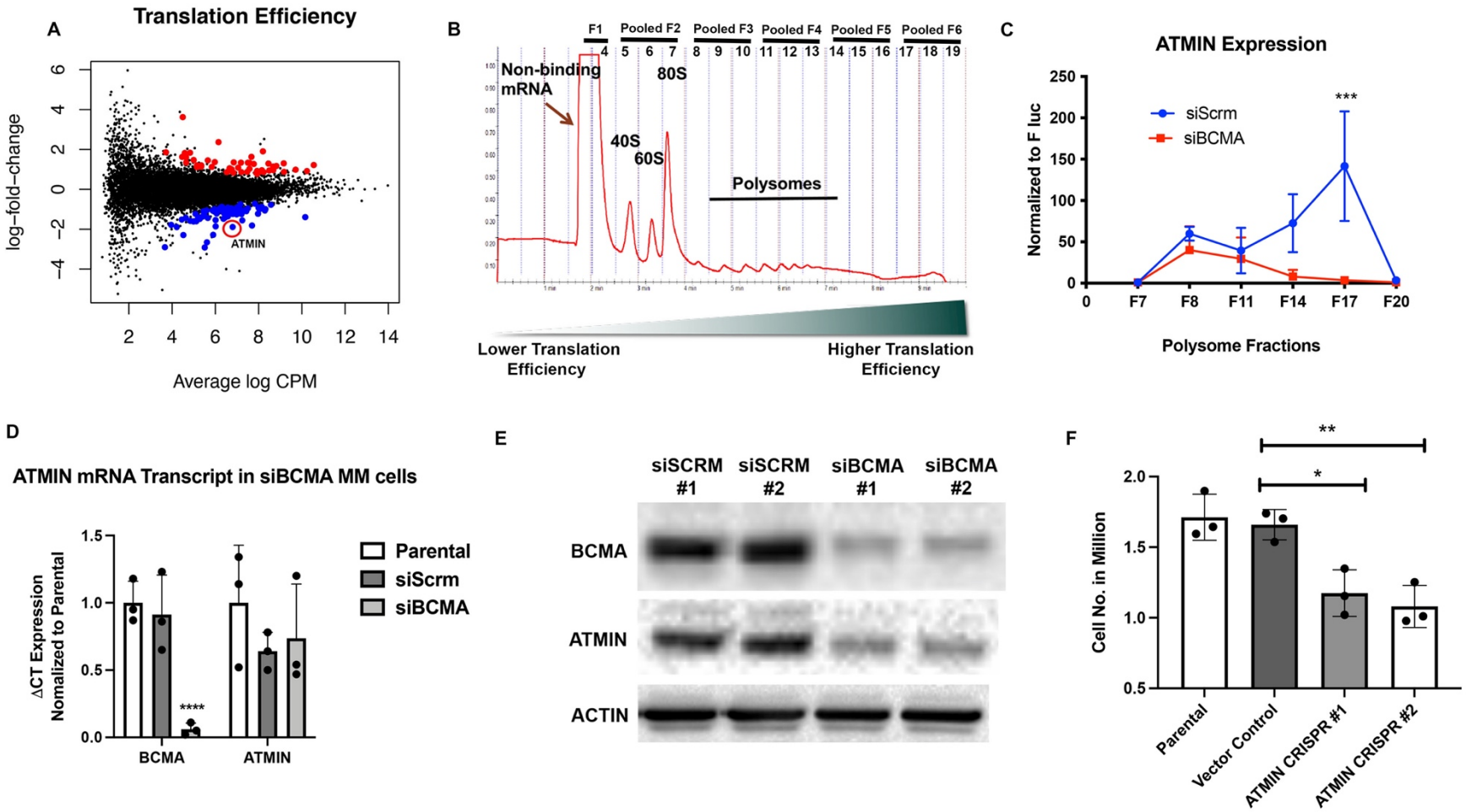
A
Translation Efficiency
log−fold−change
Average log CPM
ATMIN
B
F1
Pooled F2
Pooled F3
Pooled F4
Pooled F5
Pooled F6
Non-binding mRNA
40S
60S
80S
Polysomes
Lower Translation Efficiency
Higher Translation Efficiency
C
ATMIN Expression
Normalized to F luc
siScrm
siBCMA
Polysome Fractions
D
ATMIN mRNA Transcript in siBCMA MM cells
ΔCT Expression Nomalized to Parental
Parental
siScrm
siBCMA
BCMA
ATMIN
E
siSCRM #1
siSCRM #2
siBCMA #1
siBCMA #2
BCMA
ATMIN
ACTIN
F
Cell No. in Million
Parental
Vector Control
ATMIN CRISPR #1
ATMIN CRISPR #2

Figure 6: BCMA signaling regulates ATMIN expression by modulating translation efficiency. (A) Translation Efficiency analysis of MM cells upon loss of BCMA expression in MM. Significant events are colored in blue (downregulating) and red (upregulating) with ATMIN highlighted with red circle. **(B)** Representative polysome profile of MM cells fractionated by ultracentrifugation through a 10%-50% sucrose gradient. Fractions were pooled for mRNA analysis. **(C)** Relative abundance of ATMIN mRNA expression analyzed in each of the pooled polysome fraction comparing siSCRM with siBCMA MM cells. Each biological sample were performed in triplicates. **(D)** Total mRNA expression of BCMA and ATMIN examined in parental, siSCRM and siBCMA U266 cells. Each biological sample were performed in triplicates. **(E)** Western blotting analysis of ATMIN expression in siSCRM and 2 clones of siBCMA MM cells. **(F)** Cell growth analysis performed using U226 ATMIN CRISPR knockout MM cells. Statistical analysis was conducted using T test and one way ANOVA for comparing between treatment groups. P-value *=<0.05, **=<0.01. ***=<0.001.

REFERENCES

1. Chim CS, Kumar SK, Orlowski RZ, Cook G, Richardson PG, Gertz MA, et al. Management of relapsed and refractory multiple myeloma: novel agents, antibodies, immunotherapies and beyond. *Leukemia.* 2018;32(2):252-62.
2. Durer C, Durer S, Lee S, Chakraborty R, Malik MN, Rafae A, et al. Treatment of relapsed multiple myeloma: Evidence-based recommendations. *Blood Rev.* 2020;39:100616.
3. Raje N, Berdeja J, Lin Y, Siegel D, Jagannath S, Madduri D, et al. Anti-BCMA CAR T-Cell Therapy bb2121 in Relapsed or Refractory Multiple Myeloma. *N Engl J Med.* 2019;380(18):1726-37.
4. Lonial S, Lee HC, Badros A, Trudel S, Nooka AK, Chari A, et al. Belantamab mafodotin for relapsed or refractory multiple myeloma (DREAMM-2): a two-arm, randomised, open-label, phase 2 study. *Lancet Oncol.* 2020;21(2):207-21.
5. Watanabe G, Tanaka N, Ohhira M, Takemura H, and Iwa T. [A successful case of supraarterial myotomy for a myocardial bridging using intra-operative ultrasound technic to locate the intramural coronary artery trees]. *Nihon Kyobu Geka Gakkai Zasshi.* 1988;36(3):411-5.
6. Cohen AD, Garfall AL, Stadtmauer EA, Melenhorst JJ, Lacey SF, Lancaster E, et al. B cell maturation antigen-specific CAR T cells are clinically active in multiple myeloma. *J Clin Invest.* 2019;129(6):2210-21.
7. Zhao WH, Liu J, Wang BY, Chen YX, Cao XM, Yang Y, et al. A phase 1, open-label study of LCAR-B38M, a chimeric antigen receptor T cell therapy directed against B cell maturation antigen, in patients with relapsed or refractory multiple myeloma. *J Hematol Oncol.* 2018;11(1):141.
8. Eaton JS, Miller PE, Mannis MJ, and Murphy CJ. Ocular Adverse Events Associated with Antibody-Drug Conjugates in Human Clinical Trials. *J Ocul Pharmacol Ther.* 2015;31(10):589-604.
9. Gardeney H, Bobin A, Gruchet C, Sabirou F, Levy A, Nsiala L, et al. Three Drug Combinations in the Treatment of Fit Elderly Multiple Myeloma Patients. *J Clin Med.* 2020;9(11).
10. Elnair R, and Holstein S. Treatment Considerations for Transplant-Ineligible Multiple Myeloma. *Oncology (Williston Park).* 2021;35(4):170-82.
11. O'Connor BP, Raman VS, Erickson LD, Cook WJ, Weaver LK, Ahonen C, et al. BCMA is essential for the survival of long-lived bone marrow plasma cells. *J Exp Med.* 2004;199(1):91-8.
12. Chiu A, Xu W, He B, Dillon SR, Gross JA, Sievers E, et al. Hodgkin lymphoma cells express TACI and BCMA receptors and generate survival and proliferation signals in response to BAFF and APRIL. *Blood.* 2007;109(2):729-39.
13. Xu S, and Lam KP. B-cell maturation protein, which binds the tumor necrosis factor family members BAFF and APRIL, is dispensable for humoral immune responses. *Mol Cell Biol.* 2001;21(12):4067-74.
14. Lee L, Bounds D, Paterson J, Herledan G, Sully K, Seestaller-Wehr LM, et al. Evaluation of B cell maturation antigen as a target for antibody drug conjugate mediated cytotoxicity in multiple myeloma. *Br J Haematol.* 2016;174(6):911-22.
15. Tai YT, Mayes PA, Acharya C, Zhong MY, Cea M, Cagnetta A, et al. Novel anti-B-cell maturation antigen antibody-drug conjugate (GSK2857916) selectively induces killing of multiple myeloma. *Blood.* 2014;123(20):3128-38.

16. Tai YT, Acharya C, An G, Moschetta M, Zhong MY, Feng X, et al. APRIL and BCMA promote human multiple myeloma growth and immunosuppression in the bone marrow microenvironment. *Blood.* 2016;127(25):3225-36.
17. Moreaux J, Legouffe E, Jourdan E, Quittet P, Reme T, Lugagne C, et al. BAFF and APRIL protect myeloma cells from apoptosis induced by interleukin 6 deprivation and dexamethasone. *Blood.* 2004;103(8):3148-57.
18. Tai YT, and Anderson KC. B cell maturation antigen (BCMA)-based immunotherapy for multiple myeloma. *Expert Opin Biol Ther.* 2019;19(11):1143-56.
19. Xu S, and Lam KP. Transmembrane Activator and CAML Interactor (TACI): Another Potential Target for Immunotherapy of Multiple Myeloma? *Cancers (Basel).* 2020;12(4).
20. Briones J, Timmerman JM, Hilbert DM, and Levy R. BLyS and BLyS receptor expression in non-Hodgkin's lymphoma. *Exp Hematol.* 2002;30(2):135-41.
21. Yu G, Boone T, Delaney J, Hawkins N, Kelley M, Ramakrishnan M, et al. APRIL and TALL-I and receptors BCMA and TACI: system for regulating humoral immunity. *Nat Immunol.* 2000;1(3):252-6.
22. Castigli E, Scott S, Dedeoglu F, Bryce P, Jabara H, Bhan AK, et al. Impaired IgA class switching in APRIL-deficient mice. *Proc Natl Acad Sci U S A.* 2004;101(11):3903-8.
23. Pan-Hammarstrom Q, Salzer U, Du L, Bjorkander J, Cunningham-Rundles C, Nelson DL, et al. Reexamining the role of TACI coding variants in common variable immunodeficiency and selective IgA deficiency. *Nat Genet.* 2007;39(4):429-30.
24. Barratt J, Tumlin JA, Suzuki Y, Kao A, Aydemir A, Zima Y, et al. MO039THE 24-WEEK INTERIM ANALYSIS RESULTS OF A RANDOMIZED, DOUBLE-BLIND, PLACEBO-CONTROLLED PHASE II STUDY OF ATACICEPT IN PATIENTS WITH IGA NEPHROPATHY AND PERSISTENT PROTEINURIA. *Nephrology Dialysis Transplantation.* 2020;35(Supplement_3).
25. Klein B, Tarte K, Jourdan M, Mathouk K, Moreaux J, Jourdan E, et al. Survival and proliferation factors of normal and malignant plasma cells. *Int J Hematol.* 2003;78(2):106-13.
26. Suematsu S, Matsuda T, Aozasa K, Akira S, Nakano N, Ohno S, et al. IgG1 plasmacytosis in interleukin 6 transgenic mice. *Proc Natl Acad Sci U S A.* 1989;86(19):7547-51.
27. Bataille R, Jourdan M, Zhang XG, and Klein B. Serum levels of interleukin 6, a potent myeloma cell growth factor, as a reflect of disease severity in plasma cell dyscrasias. *J Clin Invest.* 1989;84(6):2008-11.
28. Stephens OW, Zhang Q, Qu P, Zhou Y, Chavan S, Tian E, et al. An intermediate-risk multiple myeloma subgroup is defined by sIL-6r: levels synergistically increase with incidence of SNP rs2228145 and 1q21 amplification. *Blood.* 2012;119(2):503-12.
29. Fragioudaki M, Tsirakis G, Pappa CA, Aristeidou I, Tsioutis C, Alegakis A, et al. Serum BAFF levels are related to angiogenesis and prognosis in patients with multiple myeloma. *Leuk Res.* 2012;36(8):1004-8.
30. Bolkun L, Lemancewicz D, Jablonska E, Kulczynska A, Bolkun-Skornicka U, Kloczko J, et al. BAFF and APRIL as TNF superfamily molecules and angiogenesis parallel progression of human multiple myeloma. *Ann Hematol.* 2014;93(4):635-44.
31. Tai YT, Li XF, Breitkreutz I, Song W, Neri P, Catley L, et al. Role of B-cell-activating factor in adhesion and growth of human multiple myeloma cells in the bone marrow microenvironment. *Cancer Res.* 2006;66(13):6675-82.

32. Collier FC, and Jackson P. The precipitin test for Bence-Jones protein. *N Engl J Med.* 1953;248(10):409-14.
33. Leipold D, and Prabhu S. Pharmacokinetic and Pharmacodynamic Considerations in the Design of Therapeutic Antibodies. *Clin Transl Sci.* 2019;12(2):130-9.
34. Pelletier M, Thompson JS, Qian F, Bixler SA, Gong D, Cachero T, et al. Comparison of soluble decoy IgG fusion proteins of BAFF-R and BCMA as antagonists for BAFF. *J Biol Chem.* 2003;278(35):33127-33.
35. Rennert P, Schneider P, Cachero TG, Thompson J, Trabach L, Hertig S, et al. A soluble form of B cell maturation antigen, a receptor for the tumor necrosis factor family member APRIL, inhibits tumor cell growth. *J Exp Med.* 2000;192(11):1677-84.
36. Majithia N, Vincent Rajkumar S, Lacy MQ, Buadi FK, Dispenzieri A, Gertz MA, et al. Outcomes of primary refractory multiple myeloma and the impact of novel therapies. *Am J Hematol.* 2015;90(11):981-5.
37. Kumar SK, Dispenzieri A, Fraser R, Mingwei F, Akpek G, Cornell R, et al. Early relapse after autologous hematopoietic cell transplantation remains a poor prognostic factor in multiple myeloma but outcomes have improved over time. *Leukemia.* 2018;32(4):986-95.
38. Ingolia NT, Lareau LF, and Weissman JS. Ribosome profiling of mouse embryonic stem cells reveals the complexity and dynamics of mammalian proteomes. *Cell.* 2011;147(4):789-802.
39. Ozadam H, Geng M, and Cenik C. RiboFlow, RiboR and RiboPy: an ecosystem for analyzing ribosome profiling data at read length resolution. *Bioinformatics.* 2020;36(9):2929-31.
40. Cenik C, Cenik ES, Byeon GW, Grubert F, Candille SI, Spacek D, et al. Integrative analysis of RNA, translation, and protein levels reveals distinct regulatory variation across humans. *Genome Res.* 2015;25(11):1610-21.
41. Rapali P, Garcia-Mayoral MF, Martinez-Moreno M, Tarnok K, Schlett K, Albar JP, et al. LC8 dynein light chain (DYNLL1) binds to the C-terminal domain of ATM-interacting protein (ATMIN/ASCIZ) and regulates its subcellular localization. *Biochem Biophys Res Commun.* 2011;414(3):493-8.
42. Jurado S, Gleeson K, O'Donnell K, Izon DJ, Walkley CR, Strasser A, et al. The Zinc-finger protein ASCIZ regulates B cell development via DYNLL1 and Bim. *J Exp Med.* 2012;209(9):1629-39.
43. Jurado S, Conlan LA, Baker EK, Ng JL, Tenis N, Hoch NC, et al. ATM substrate Chk2-interacting Zn2+ finger (ASCIZ) Is a bi-functional transcriptional activator and feedback sensor in the regulation of dynein light chain (DYNLL1) expression. *J Biol Chem.* 2012;287(5):3156-64.
44. Leszczynska KB, Gottgens EL, Biasoli D, Olcina MM, Ient J, Anbalagan S, et al. Mechanisms and consequences of ATMIN repression in hypoxic conditions: roles for p53 and HIF-1. *Sci Rep.* 2016;6:21698.
45. Becker JR, Cuella-Martin R, Barazas M, Liu R, Oliveira C, Oliver AW, et al. The ASCIZ-DYNLL1 axis promotes 53BP1-dependent non-homologous end joining and PARP inhibitor sensitivity. *Nat Commun.* 2018;9(1):5406.
46. McNees CJ, Conlan LA, Tenis N, and Heierhorst J. ASCIZ regulates lesion-specific Rad51 focus formation and apoptosis after methylating DNA damage. *EMBO J.* 2005;24(13):2447-57.

47. Jurado S, Smyth I, van Denderen B, Tenis N, Hammet A, Hewitt K, et al. Dual functions of ASCIZ in the DNA base damage response and pulmonary organogenesis. *PLoS Genet.* 2010;6(10):e1001170.
48. Rossi JF, Moreaux J, Hose D, Requirand G, Rose M, Rouille V, et al. Atacicept in relapsed/refractory multiple myeloma or active Waldenstrom's macroglobulinemia: a phase I study. *Br J Cancer.* 2009;101(7):1051-8.
49. Moreaux J, Hose D, Jourdan M, Reme T, Hundemer M, Moos M, et al. TACI expression is associated with a mature bone marrow plasma cell signature and C-MAF overexpression in human myeloma cell lines. *Haematologica.* 2007;92(6):803-11.
50. Schuepbach-Mallepell S, Das D, Willen L, Vigolo M, Tardivel A, Lebon L, et al. Stoichiometry of Heteromeric BAFF and APRIL Cytokines Dictates Their Receptor Binding and Signaling Properties. *J Biol Chem.* 2015;290(26):16330-42.
51. Marsters SA, Yan M, Pitti RM, Haas PE, Dixit VM, and Ashkenazi A. Interaction of the TNF homologues BLyS and APRIL with the TNF receptor homologues BCMA and TACI. *Curr Biol.* 2000;10(13):785-8.
52. Wu Y, Bressette D, Carrell JA, Kaufman T, Feng P, Taylor K, et al. Tumor necrosis factor (TNF) receptor superfamily member TACI is a high affinity receptor for TNF family members APRIL and BLyS. *J Biol Chem.* 2000;275(45):35478-85.
53. Ingolia NT, Hussmann JA, and Weissman JS. Ribosome Profiling: Global Views of Translation. *Cold Spring Harb Perspect Biol.* 2019;11(5).
54. Perini T, Materozzi M, and Milan E. The Immunity-malignancy equilibrium in multiple myeloma: lessons from oncogenic events in plasma cells. *FEBS J.* 2021.
55. Pawlyn C, and Jackson GH. Physicians, paraproteins and progress: diagnosis and management of myeloma. *Br J Hosp Med (Lond).* 2019;80(2):91-8.
56. Rodriguez JM, Rodriguez-Rivas J, Di Domenico T, Vazquez J, Valencia A, and Tress ML. APPRIS 2017: principal isoforms for multiple gene sets. *Nucleic Acids Res.* 2018;46(D1):D213-D7.
57. Robinson MD, and Oshlack A. A scaling normalization method for differential expression analysis of RNA-seq data. *Genome Biol.* 2010;11(3):R25.
58. Kassambara A, and Moreaux J. Analysis of Global Gene Expression Profiles. *Methods Mol Biol.* 2018;1792:157-66.